Advances in Aircraft and Spacecraft Science, *Vol. 2, No. 3 (2015) 263-273*
DOI: http://dx.doi.org/10.12989/aas.2015.2.3.263

Modeling of an embedded carbon nanotube based composite strain sensor

M. Boehle*[1], P. Pianca[1], K. Lafdi[1] and F. Chinesta[2]

[1]*University of Dayton Research Institute, 300 College Park, Dayton, OH 45469, USA*
[2]*Ecole Centrale of Nantes, 1 rue de la Noe, BP 92101, 44321 Nantes cedex 3, France*

(Received August 6, 2014, Revised October 6, 2014, Accepted October 14, 2014)

Abstract. Carbon nanotube strain sensors, or so called "fuzzy fiber" sensors have not yet been studied sufficiently. These sensors are composed of a bundle of fiberglass fibers coated with CNT through a thermal chemical vapor deposition process. The characteristics of these fuzzy fiber sensors differ from a conventional nanocomposite in that the CNTs are anchored to a substrate fiber and the CNTs have a preferential orientation due to this bonding to the substrate fiber. A numerical model was constructed to predict the strain response of a composite with embedded fuzzy fiber sensors in order to compare result with the experimental results obtained in an earlier study. A comparison of the numerical and experimental responses was conducted based on this work. The longitudinal sensor output from the model matches nearly perfectly with the experimental results. The transverse and off-axis tests follow the correct trends; however the magnitude of the output does not match well with the experimental data. An explanation of the disparity is proposed based on microstructural interactions between individual nanotubes within the sensor.

Keywords: carbon nanotubes; fuzzy fiber; strain sensing; Structural Health Monitoring (SHM); nanocomposite

1. Introduction

The strain sensing abilities of carbon nanotubes (CNT) in various formulations have been studied exhaustively. The most often studied formulation being some type of nanocomposite film or ink composed of dispersed carbon nanomaterials in a polymer matrix (Li *et al*. 2008, Li and Chou 2008, Thostenson and Chou 2008, Alexopoulos 2010, Barber *et al*. 2004, Rausch and Mäder 2010). The strain sensing behavior of such nanocomposites have been studied in depth. Their piezoresistive behavior and tunneling effect are very well understood.

Prior studies of the strain sensing abilities of "fuzzy fiber" CNT sensors have shown a linear and reversible electrical response to applied strain. Studies have been performed both on single fibers (Boehle *et al*. 2012) and on bundles of fibers, as used in the current work (Sebastian *et al*. 2014). The electrical response is suspected to be predominantly due to the piezoresistance of the CNTs with the tunneling effect playing some part as well. These phenomena have been studied quite thoroughly in polymer nanocomposites (Karimov *et al*. 2012, Kang *et al*. 2006, Vemuru *et*

*Corresponding author, Ph.D., E-mail: matthew.boehle@udri.udayton.edu

http://www.techno-press.org/?journal=aas&subpage=7 ISSN: 2287-528X (Print), 2287-5271 (Online)

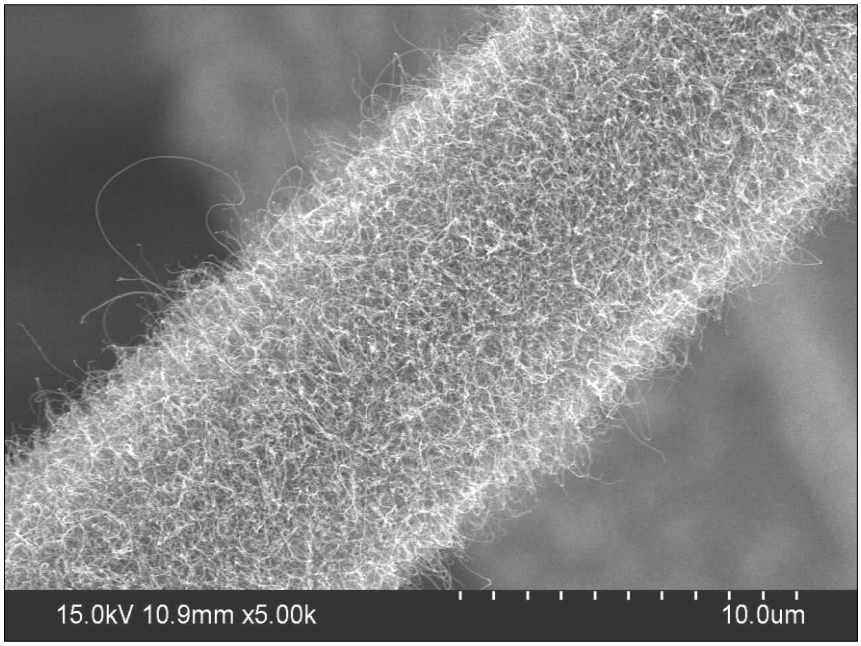

Fig. 1 SEM micrograph of CNT growth on fiber

al. 2009, Thostenson and Chou 2008, Grow *et al*. 2005, Alamusi *et al*. 2011, Dharap *et al*. 2004, Hu *et al*. 2008, Hu *et al*. 2010, Hu *et al*. 2013, Abot *et al*. 2010). It is suspected that the tunneling effect plays a minor role in the electrical response due to the orientation of the CNTs and their intimate contact with neighboring CNTs. Some response may be from the strain induced change in the direct CNT to CNT contact established when the sensor was made.

A test specimen with a special geometry was constructed to allow characterization of the fuzzy fiber sensor under various mechanical loads. Sensors were loaded in tension, compression and shear to quantify the response of the sensor to specific strain orientations and to assess whether the response was due to Poisson's effect or if there was another dominant response mode. Current manufacturing abilities do not allow tight control of sensor properties so the special specimen geometry was fabricated to allow testing sensors in multiple loading cases within a single specimen.

A numerical finite element (FE) model was constructed to better understand the fiber response. A key task is to develop a relationship to translate the sensor response to true strain so that the sensor can be used to monitor strain. The FE model was constructed to replicate the experimental specimen in composition and sensor placement. To simplify the model, the sensors were assumed to be a single homogeneous fiber with cross-section and properties chosen to replicate the actual sensor. Modeling the inter-CNT phenomena was outside the scope of this effort.

2. Test specimen construction

Each sensor was comprised of approximately 3000 fiberglass filaments each coated with CNTs. The nanotube coating is obtained by applying a catalyst to the surface of the fibers and then performing a thermal chemical vapor deposition (CVD) process to grow the nanotubes. Fig. 1

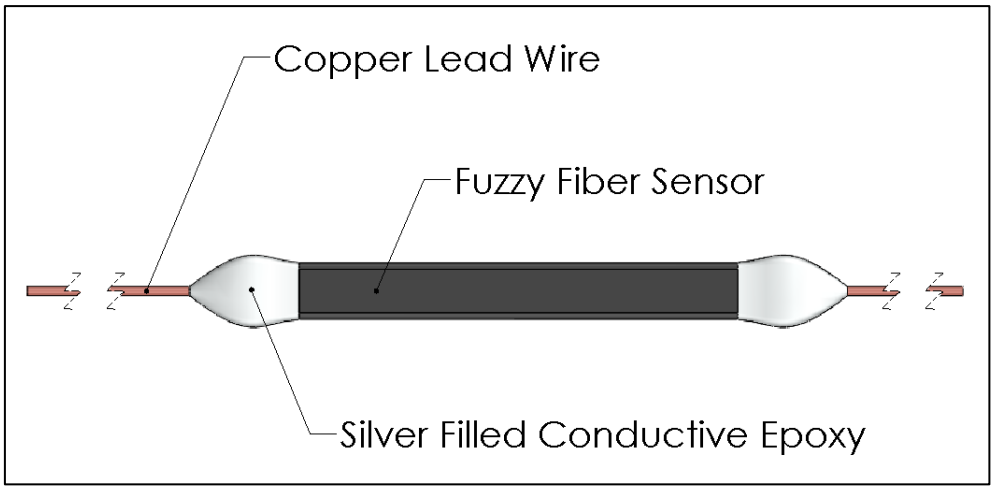

Fig. 2 Illustration of fuzzy fiber sensor

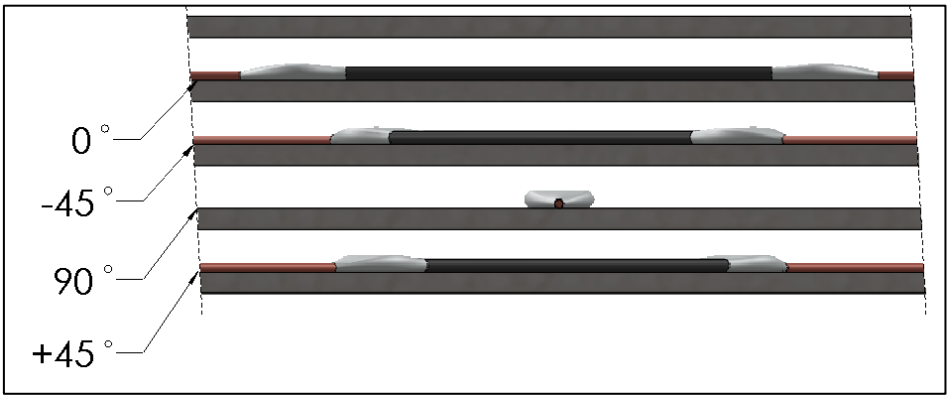

Fig. 3 Illustration of sensor placement within composite panel

shows a micrograph of a typical fiber taken from a fuzzy fiber sensor. The fuzzy fiber bundles are turned into sensors by attaching copper lead wires. This is accomplished with silver filled epoxy. The conductive epoxy provides a low impedance connection between the copper lead wire, which extends out the edge of the specimen, and the sensor itself. Fig. 2 shows an illustration of a sensor ready for use. Small diameter heat shrink tubing was placed around the lead wires where they exit the specimen to prevent breakage due to mechanical stress on the small diameter wires.

To investigate sensor response to longitudinal, transverse, and off-axis loading conditions, a unique specimen was fabricated from randomly-oriented chopped strand fiberglass mat and E-862 Epoxy. The randomly-oriented fiber provided a quasi-isotropic planar specimen which minimized any possible influences of fiber directionality on sensor response. The 11-ply specimen contained 4 independent sensors of 25 mm gage length, each at different layers and orientations in the laminate. The sensors were located in the center of the laminate, each being separated by one layer of fiberglass to provide electrical isolation. Fig. 3 shows an illustration of the panel layup, with the top three and bottom three layers hidden for clarity.

The specimen was fabricated as a square panel using the resin film infusion (RFI) process. As

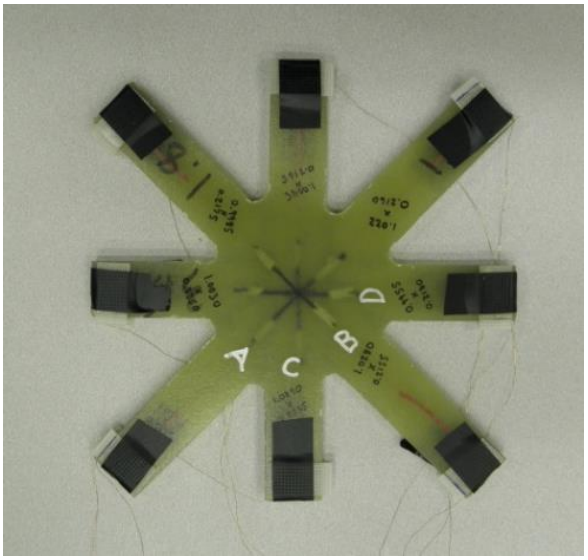

Fig. 4 Sensor-orientation specimen machined and ready for testing

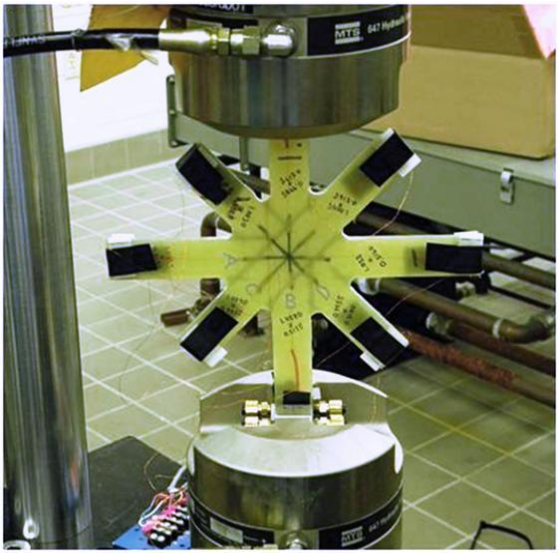

Fig. 5 Sensor-orientation specimen loaded into test machine

each layer was placed, the assembled sensors were placed inside the layup. The panel was autoclave cured after layup was completed. A diamond wet saw was used to cut the final specimen shape from the square panel. The fillet radius between each arm was accomplished with a diamond coated hole saw with 13 mm diameter. Each leg of the specimen had nominal width and thickness of 25 mm and 5 mm, respectively. The fabricated and machined specimen is shown in Fig. 4. Fig. 5 shows the specimen loaded into the hydraulic test machine ready for testing with load applied in the "B" direction.

3. Instrumentation and testing

Connections to the sensors were made with copper lead wires and conductive silver filled epoxy prior to layup and cure of the test specimen. The sensors were monitored with a Wheatstone bridge circuit, as is traditionally done with a metal foil strain gage. A Vishay 2310 signal conditioner with a gain of 100 was used to amplify the sensor response, and bridge excitation was set to 10 V, with no concerns with self-heating due to the large (>1 kΩ) resistance of the sensors. The nominal resistance of these sensors was near 3 kΩ.

The specimen was tested in an MTS servohydraulic load frame with hydraulic wedge grips and a digital controller. In addition to load and displacement data, the controller was able record three more analog signals. A reference extensometer was not used to allow three channels of sensor data to be collected simultaneously.

Tests were run dynamically, with a triangle wave of 0 to 4.45kN applied at 0.3 and 0.03 Hz. This load was applied to opposite arms of the specimen, while sensor response was monitored in three of the four possible directions. The wheatstone bridge for each sensor was zeroed to provide zero output when the load was at half scale (2.225 kN) in order to maximize dynamic range within the -10 to +10V range of the signal conditioner. In order to cancel any effects from sensor location

or fabrication, the test sequence was structured so that three channels were connected and, then, the response was recorded to load applied across each of the four sets of arms. One amplifier was moved to the previously unmonitored channel and the test sequence was repeated, providing four channels of sensor data for each of four loading directions.

A thorough presentation and analysis of the experimental test results can be found in prior work presented in Reference 8. Experimental testing is briefly covered here to provide some explanation of how the testing was performed. A complete analysis is not repeated here for the sake of brevity.

4. Modelling and results

A finite element model was constructed to corroborate the experimental data. Abaqus/CAE software was used to construct the model, which is shown in Fig. 6. To reduce calculation time, only half of the thickness of the specimen was modeled. The boundary conditions and material properties were set to mimic those of the experimental test. As is evident from the model in Fig. 3, the six legs of the specimen which are not loaded are under very little stress. In order to simplify the model and refine the mesh near the sensors, the model was trimmed to focus on the part of the model where the stresses were highest. Fig. 7 shows this modified model with inactive arms removed and a fine mesh around the sensor areas.

The goal of the modeling is to attempt to backup and explain the experimental data. The result sought is to monitor the change of resistance of the sensors and use those values to calculate the

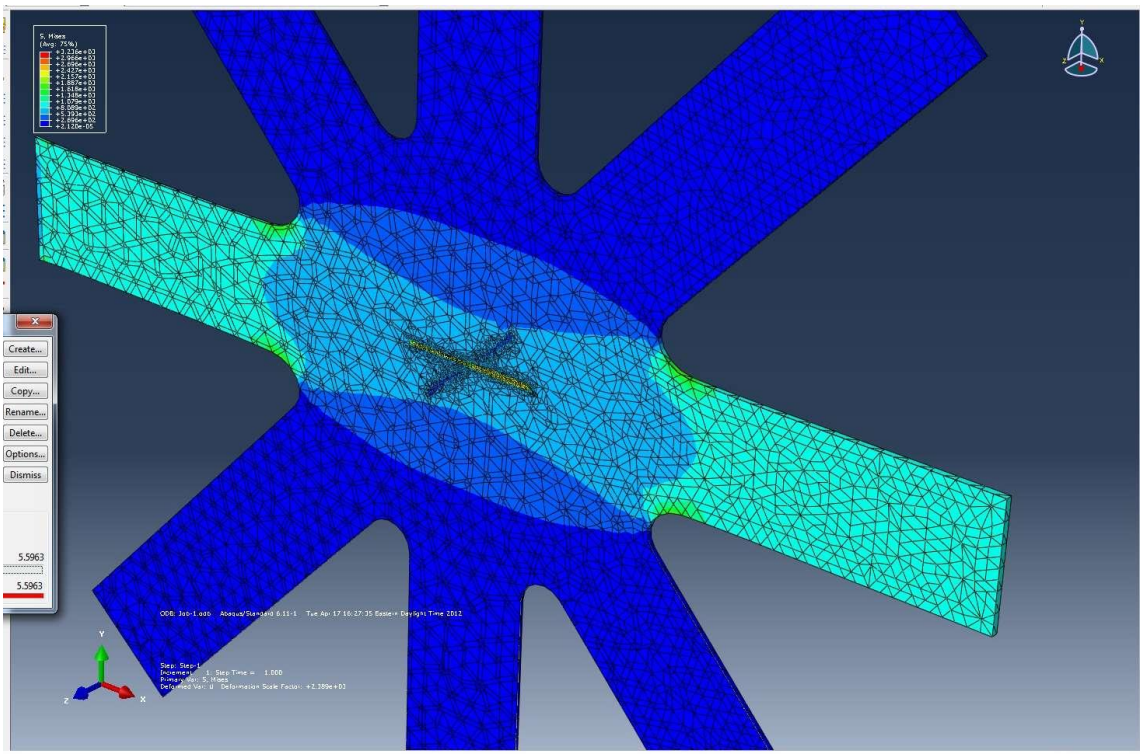

Fig. 6 Initial FE model following specimen design

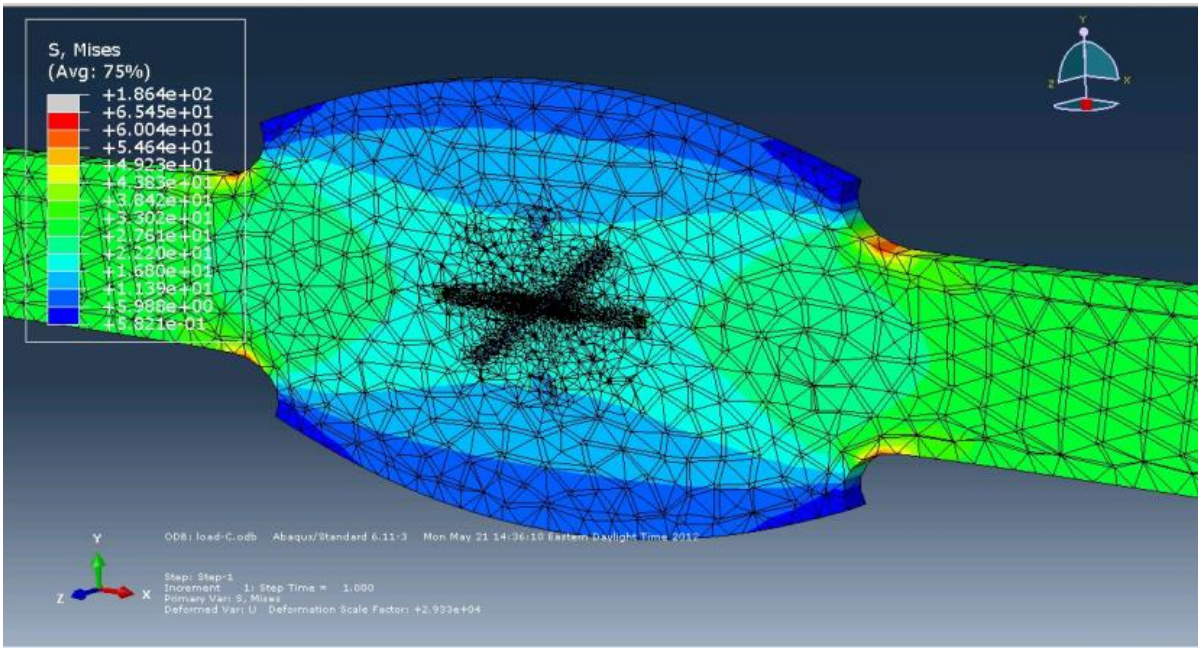

Fig. 7 Refined FE model with inactive portions removed

expected wheatstone bridge output, so that the model can be compared with the experimental data.

The physical phenomenon of the change of resistance is not yet fully known and would be cumbersome to model accurately. It involves the flexure and changing contact between millions of CNTs, in a complex, entangled network on the surface of the fiber. Previous tests showed that the resistance of the fuzzy fiber sensor varies linearly with the strain when loaded in pure tension (Li *et al*. 2008, Li and Chou 2008). Consequently, it was assumed in the model that the sensor's resistance change should be calculated based on the strain along the longitudinal axis of the sensor, independent of the loading direction. A linear correspondence law was used.

For the model, the specimen was assumed to have isotropic properties in the plane. To simplify the model, the same properties were assumed in the *z* direction. We know this is not true in practice but it is a safe assumption in this case because there is very little *Z* axis stress. This assumption allowed treating the specimen as an isotropic and homogeneous linear elastic material. The Young's modulus was set to 8 GPa to follow published test results of similar random orientation glass fiber reinforced plastics.

In this specimen, the sensors are stiffer than the surrounding material due to the random orientation in the specimen and the uniaxial orientation within the sensor. The Young's modulus was set to 70 GPa (the tensile modulus of glass fiber) in the model to reflect this. The four sensors are each made out of a fuzzy fiber tow composed of approximately 3000 filaments with a diameter of 7 μm. As it is not realistically possible to represent each filament in a FE model, the tow was assumed as one equivalent isotropic linear elastic fiber, with the same cross section as the 3000 filaments together. The sensor exhibits an elliptical cross-section due to being sandwiched inside the specimen and cured under pressure in an autoclave. Each sensor was separated from the next by 1 ply, each about 0.5 mm thick. The length of the sensor was set equal to the length between the two silver points connectors (25 mm) in the specimen. This is the active length of the sensor.

The interfacial bond between the sensors and the composites was modeled with a complete six degree of freedom constraint between the shared nodes of the interface surface. In order to achieve this bond, the sensor geometry is modeled as cells with different material properties inside the composite solid. This method allows the meshes to correspond across the interface

Quadratic tetrahedron elements were selected to accommodate the curved shapes, especially near the interfaces of the sensors. When meshing, Abaqus first creates linear tetrahedrons, and then transforms them into quadratic elements.

Sizing control is set in order to get mesh elements of 4mm minimum approximate global size for the GFRP, and 1.7 mm minimum for the sensors. The mesh surrounding the sensors will be further refined by dividing the sensors in 25 cells, resulting in elements of 0.05 mm approximate size. The sensor being in the main load direction will be meshed with a 0.5 mm sizing control, resulting in an even more refined mesh, but a quick mesh sensitivity study will prove that this does not have any significant impact on the result. It will be verified that the elements are small enough so that there is no more than 1/10 of the Von Mises fringe stress and strain discrepancy between two adjacent elements.

The boundaries conditions are defined as a fixed constraint on the tip of one arm of the loaded direction, and a surface traction of -4445 N equivalent to 1000 Lbs load on the tip of the opposite arm. Simulation shows that the stress is well distributed inside the arms of the loaded direction, and that they are not creating any improper discontinuity.

The strain data is acquired after computation of the job by creating four paths, one for each sensor. The paths are geometric segments 25 mm long that run through the center of the sensor's cross-section. It has been verified that the stress is homogeneous along the section of the sensor, so reading the strain in the middle of it is a fair assumption in order to get its surface strain. Two reference systems are used in order to extract the strain data along the path, in regards to the direction of the fiber.

Around 300 strain data points are extracted for each path. These points are averaged over each 1mm of the path to correspond with the 25 cells composing the sensor in Abaqus. This averaged strain is used to calculate a resistance using a linear relationship. This relationship is constructed from the experimental electrical resistivity of the sensors and includes the wheatstone bridge transformation from resistance to volt output, so that bridge output voltages can be compared to experimental results. Engineering strain is defined as

$$\varepsilon = \frac{\Delta L}{L} \tag{1}$$

where ε is engineering strain, ΔL is the change in length and L is the initial length. Therefore

$$\Delta L = \varepsilon \cdot L \tag{2}$$

Poisson effects can now be calculated by introducing the concept of an equivalent sensor diameter d, which will change from its initial value by some amount ΔD which can be calculated as follows

$$\Delta D = -D \cdot \upsilon \cdot \varepsilon \tag{3}$$

where υ is the Poisson's ratio of the sensor material. The sum of ΔL and L is the length of the sensor, ℓ, under strain ε, stated as

$$\ell = \Delta L + L \tag{4}$$

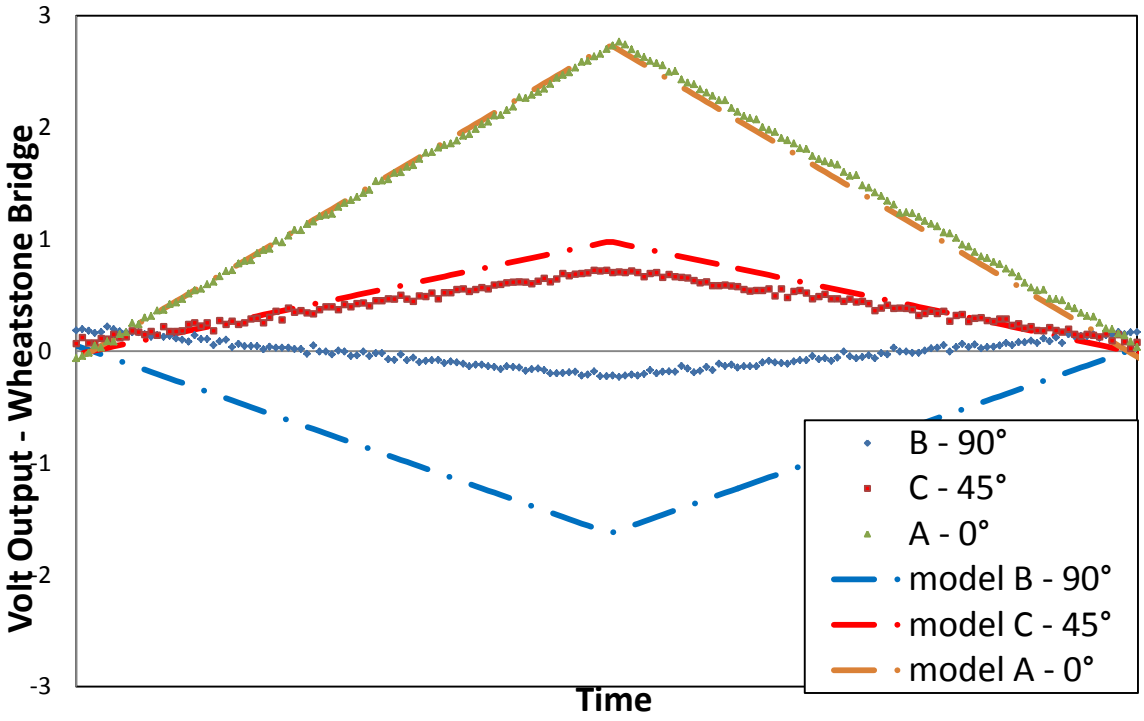

Fig. 8 FEA model and experimental results

And similarly for the equivalent diameter, d

$$d = \Delta D + D \tag{5}$$

The formula for electrical resistivity is stated as

$$R = \rho \frac{l}{A} \tag{6}$$

where R is resistance, ρ is the electrical resistivity, l is the length and A is the cross-sectional area. From Eq. (6), initial resistance (substituting L and D) and current resistance (substituting ℓ and d) can be calculated

$$Ri = \rho \frac{4L}{\pi D^2} \tag{7}$$

$$R = \rho \frac{4\ell}{\pi d^2} \tag{8}$$

where R_i is the initial resistance of the sensor and R is the resistance of the sensor with applied strain, ε. A wheatstone bridge voltage output can be calculated as follows

$$V_{out} = \left(\frac{R_2}{R_1 + R_2} - \frac{R}{R + R_3} \right) \cdot V_S \tag{9}$$

which reduces to

$$V_{out} = \left(0.5 - \frac{R}{R + R_b} \right) \cdot V_S \tag{10}$$

when a single active resistor is used, where V_{out} is the output voltage, R_b is a bridge balancing resistor and V_S is the applied voltage to the wheatstone bridge. Eq. (10) can be used to construct a plot of model response (calculated from strain values extracted from the model) to compare to experimental wheatstone bridge output values recorded previously.

Fig. 8 shows the comparison between the experimental results and the model for one loading case. Other loading cases provided similar responses to that of Fig. 8. The experimental data is extracted from a cyclic loading case wherein the tensile load is varied from 0 to 4.45 kN. The half cycle shown is from half load to maximum load and then back to half load. The longitudinal (0°) response of the model was scaled based on the experimental results. The off-axis (+/-45°) response predicted by the model was slightly higher than the experimental result and the transverse (90°) response was much higher (~600%) in the model than what was found in the experimental testing. It is suspected that the fuzzy fiber material exhibits a different response to tensile and compressive loading which is not accounted for in the model. Since the nanotubes are normal to the surface of the fiber and in close proximity and tightly packed, the change in the conductive path of the sensor is large when the nanotubes are spread apart under tensile loading. The response to compressive loading is much smaller due to the dense nature of the conductive nanotube network.

5. Conclusions

The longitudinal sensor output from the model matches nearly perfectly with the mechanical test results. The peak values are the same because the model was normalized to match the experimental data. Both the model and the experiment show linear responses to stresses in each loading case. The transverse and off-axis tests follow the correct trends; however the magnitude of the output does not match well with the experimental data. The model is currently being enhanced to investigate shear sensitivity, which may correct the error in the off-axis fiber response.

The experimental transverse response is much smaller than the model predicts. It is suspected that the response of the fuzzy fiber to transverse loading is governed by a different mechanism than the longitudinal result. The model has assumed a purely piezoresistive effect with similar sensitivities to tensile and compressive strain, which obviously does not adequately fit the actual sensor behavior. The complex microstructure of the sensor may explain the difference in sensitivities. The closely packed conductive nanotube network may be easily stretched apart, but cannot be easily compressed and so has a lower sensitivity to compressive strain. This phenomenon can be visualized with a Slinky or Jacob's ladder toy. Each can be easily pulled apart, but cannot be compressed further once in their relaxed state. Further work will be performed to investigate shear sensitivity and orthotropic sensitivity of the fuzzy fiber sensor to various loading conditions.

The efforts presented here highlight the feasibility of incorporating carbon nanomaterials into structural composites as sensors. The CNT covered glass fiber has been shown to be a viable alternative to conventional metal foil strain gages. The fuzzy fiber sensors exhibit similar sensitivity to conventional strain gages and are more easily integrated into composite structures as

the sensor itself is a composite. The fuzzy fiber strain gages can be used to sense strain within composite structures and can be readily integrated into the structural laminate to provide sensing over large sections and in locations not accessible to conventional strain gauging techniques.

The unique properties of the CNT covered fuzzy fiber lends itself to application in a wide range of sensing tasks within a structural composite including strain, temperature, degradation, etc. The fuzzy fiber may be tailored so that the same sensor can be used for a multitude of sensing applications. The sensitivity of the fuzzy fiber to a certain stimulus can be amplified by its application so that the sensor will sense the desired parameter, without significant cross talk from other stimuli the sensor may be inherently susceptible to.

Acknowledgements

This research was carried out under AFOSR Award No. FA9550-09-1-0686 and ONR Award No. N00014-13-1-0110. The authors would like to thank Tom Whitney and Peter Phillips from The University of Dayton Research Institute for their support in methodology and modeling of the star specimen.

References

Abot, J.L., Song, Y., Vatsavaya, M.S., Medikonda, S., Kier, Z., Jayasinghe, C. *et al.* (2010), "Delamination detection with carbon nanotube thread in self-sensing composite materials", *Compos. Sci. Tech*., **70**, 1113-1.

Alexopoulos, N.D., Bartholome, C., Poulin, P. and Marioli-Riga, Z. (2010), "Damage detection of glass fiber reinforced composites using embedded PVA-carbon nanotube (CNT) fibers", *Compos. Sci. Tech*., **70**, 1733-1741.

Barber, A.H., Zhao, Q., Wagner, H.D., Baillie, C.A. (2004) "Characterization of E-glass–polypropylene interfaces using carbon nanotubes as strain sensors", *Compos. Sci. Tech*., **64**, 1915-1919.

Boehle, M., Jiang, Q., Li, L., Lagounov, A. and Lafdi, K. (2012), "Carbon nanotubes on glass fiber as a strain sensor for real time structural health monitoring", *Int. J. Smart Nano Mater*., **3**(2),162-168.

Dharap, P., Li, Z., Nagarajaiah, S., Barrera, E.V. (2004), "Nanotube film based on single-wall carbon nanotubes for strain sensing", *Nanotechnology*, **15**, 379-382.

Grow, R.J., Wang, Q., Cao, J., Wang, D. and Dai, H. (2005), "Piezoresistance of carbon nanotubes on deformable thin-film membranes", *Appl. Phys. Lett*., **86**, 93-104.

Hu, B., Hu, N., Cai, Y., Yuan, W., Yan, C., Cai, Y. *et al*. (2013), "Performance characterization of VGCF/epoxy nanocomposite sensors under static load cycles and in static structural health monitoring", *Smart Mater. Struct*., **22**, 045008-045017.

Hu, N., Fukunaga, H., Atobe, S., Liu, Y. and Li, J. (2011), "Piezoresistive Strain Sensors Made from Carbon Nanotubes Based Polymer Nanocomposites", *Sensors*, **11**, 10691-10723.

Hu, N., Karube, Y., Yan, C., Masuda, Z. and Fukunaga, H. (2008), "Tunneling effect in a polymer/carbon nanotube nanocomposite strain sensor", *Acta Materialia*, **56**, 2929-2936.

Hu, N., Karube, Y., Arai, M., Watanabe, T., Yan, C., Li, Y. *et al.* (2010), "Investigation on sensitivity of a polymer/carbon nanotube composite strain sensor", *Carbon*, **48**, 680-687.

Kang, I., Schulz, M.J., Kim, J.H., Shanov, V. and Shi, D. (2006), "A carbon nanotube strain sensor for structural health monitoring", *Smart Mater. Struct*., **15**(3), 737-748.

Karimov, K.S., Khalid, F.A. and Chani, M.T.S. (2012), "Carbon nanotubes based strain sensors. *Measurement*, **45**, 918-921.

Li, C., Thostenson, E.T. and Chou, T.W. (2008), "Sensors and actuators based on carbon nanotubes and their composites: A review", *Compos. Sci. Tech*., **68**, 1227-1249.
Li, C. and Chou, T.W. (2008), "Modeling of damage sensing in fiber composites using carbon nanotube networks", *Compos. Sci. Tech*., **68**, 3373-3379.
Rausch, J. and Mäder, E. (2010) "Health monitoring in continuous glass fibre reinforced thermoplastics: Manufacturing and application of interphase sensors based on carbon nanotubes", *Compos. Sci. Tech*., **70**, 1589-1596.
Sebastian, J., Schehl, N., Bouchard, M., Boehle, M., Li, L., Lagounov, A. and Lafdi, K. (2014), "Health monitoring of structural composites with embedded carbon nanotube coated glass fiber sensors", *Carbon*, **66**, 191-200.
Thostenson, E.T. and Chou, T.W. (2008), "Carbon nanotube-based health monitoring of mechanically fastened composite joints", *Compos. Sci. Tech*., **68**, 2557-2561.
Thostenson, E.T. and Chou, T.W. (2008), "Real-time in situ sensing of damage evolution in advanced fiber composites using carbon nanotube networks", *Nanotechnology*, **19**, 1-6.
Vemuru, S.M., Wahi, R., Nagarajaiah, S. and Ajayan, P.M. (2009), "Strain sensing using a multiwalled carbon nanotube film", *J. Strain Anal*., **44**, 555-562.

AB